Reactive Pathways Toward Parasitic Release of Singlet Oxygen in Metal-air Batteries.

Adriano Pierini,[1] Sergio Brutti[1,2] and Enrico Bodo[1,*]

[1]Department of Chemistry, University of Rome "La Sapienza", P. A. Moro 5, 00185 Rome, Italy

[2]GISEL—Centro di Riferimento Nazionale per i Sistemi di Accumulo Elettrochimico di Energia, INSTM

via G. Giusti 9, 50121 Firenze, Italy

*E-mail: enrico.bodo@uniroma1.it

Supplementary Figures

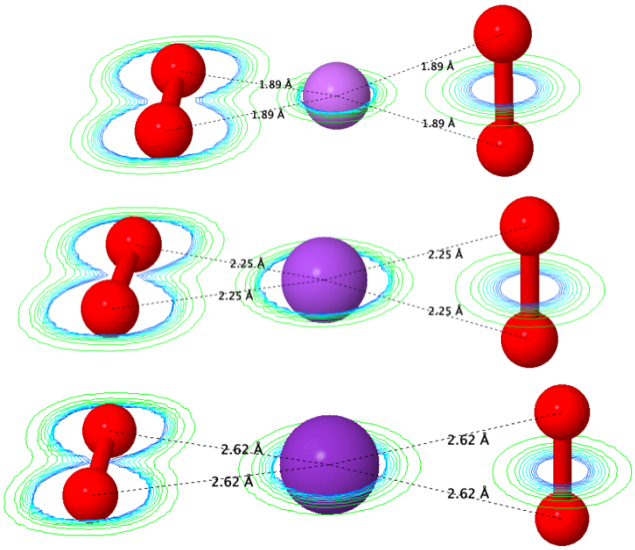

Supplementary Figure 1. MP2 optimized geometries of the superoxide complexes MO_4^- from top to bottom: Li^+, Na^+ and K^+. The M—O distances are reported to highlight the symmetry. The CASSCF(18,13) electronic density is reported on the xy plane as contours.

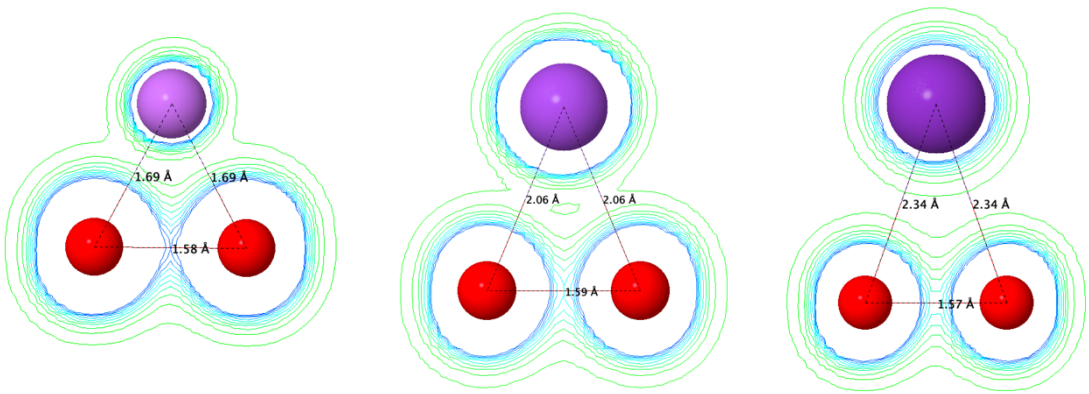

Supplementary Figure 2. MP2 optimized geometries of the peroxide complexes MO_2^- from left to right: Li^+, Na^+ and K^+. The M—O and O—O distances are reported to highlight the symmetry. The CASSCF(10,7) electronic density is reported on the xy plane as contours.

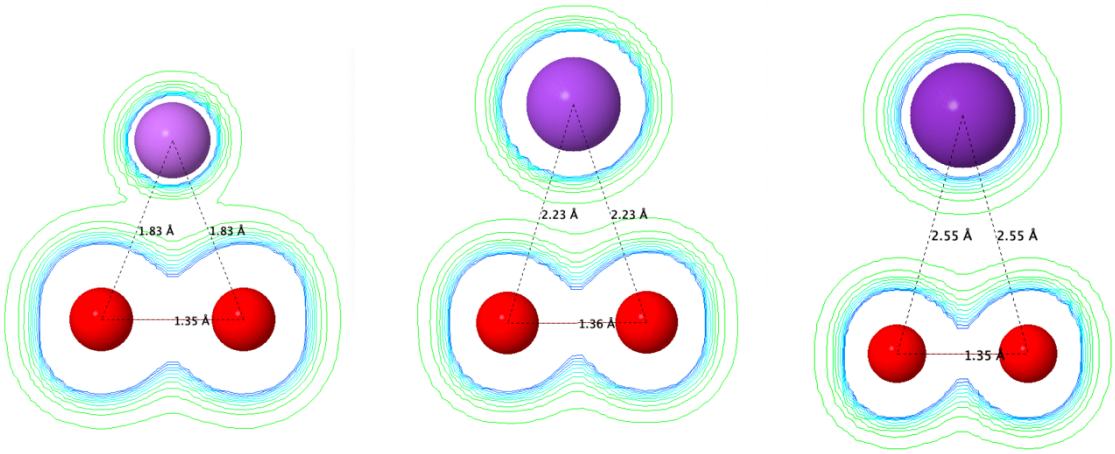

Supplementary Figure 3. MP2 optimized geometries of the superoxide complexes $M^{\nu}O_2^{-}$ from left to right: Li^+, Na^+ and K^+. The M—O and O—O distances are reported to highlight the symmetry. The CASSCF(10,7) electronic density is reported on the xy plane as contours.

Supplementary Methods

In Supplementary Table 1 we verify that, in the case of the inherently multi-reference $M^0O_2^-$ specie, the use of single-reference perturbation theory in a broken-symmetry formalism is at least able to reproduce the structural features of the open-shell singlet, yielding geometries which differ very little from the ones obtained at the NEVPT2 level (numerical gradients). CASSCF geometries instead present slightly larger deviations since the method is able to recover only a small part of dynamical correlation.
In Supplementary Table 2 we report a numerical test to check the quality of the adopted basis set (ma-def2-TZVP), comparing the results of the reaction energies involving the lithium cation in vacuum with those obtained with the ma-def2-QZVPP basis. The triplet-singlet O2 energy gap is also included.

Supplementary Discussion

We explore the effect due to the additional presence of a second metal cation. This variation takes into account the fact that the metal ions are in great excess with respect to superoxide ions. In order to keep the thermodynamic data consistent, we add a second metal cation to both the product and the reactants, hence we consider the thermodynamic of the following reaction:

$$MO_2 + MO_2 \rightarrow M_2O_2 + {}^3O_2$$

where the final M_2O_2 product can be either in its peroxide state $M^+O_2^{2-}M^+$ or in its superoxide (partially reduced) state $M^0O_2^-M^+$. The detailed results are reported in Supplementary Table 3. The main effect of the additional metal cation is to stabilize the products owing to a favorable electrostatic interaction between the added metal cation and the dioxide moiety either in its dianionic form (peroxide) or monoanionic form (superoxide). In a solvent medium, the reaction leading to the peroxide Li_2O_2 becomes globally endothermic of few hundreds of meV while the formation of Na_2O_2 and K_2O_2 remain endothermic with a consistent reduction of the reaction enthalpy down to 0.2-0.4 eV for the former and 0.6-0.8 eV for the latter. The energies of the reaction leading to the superoxide $M^0O_2^-M^+$ behaves in a different way. The presence of the second metal cation stabilizes the reactants much more than the products, hence the endothermicities of the reaction leading to the superoxide/metal reduction channel are only slightly affected with respect to those in Table 2 and turn out to lie between 1.4 and 2.3 eV depending on the specific cation and solvent model. This result seems to point to a net preference for the peroxide channel with respect to the metal reduction/superoxide one when we are in the presence of an excess of metal cations. However, due to the intrinsic limits of the computational model, it is impossible for us to assess the propensity for the ionic couples (containing the additional metal cation) to remain bound along the reaction path with solvent polarity acting against it.

Supplementary Tables

Supplementary Table 1: Geometries of the complex at the (broken symmetry) SCS-MP2 level compared to CASSCF and NEVPT2, the latter with numerical gradients.

Method	Li^+		Na^+		K^+	
	d(O-O)	d(O-M)	d(O-O)	d(O-M)	d(O-O)	d(O-M)
SCS-MP2	1.354	1.830	1.356	2.230	1.352	2.554
CASSCF	1.362	1.808	1.367	2.211	1.360	2.554
NEVPT2	1.356	1.825	1.359	2.225	1.354	2.540

Supplementary Table 2: Example of the energy differences convergence with different basis sets.

Reaction	ma-def2-TZVP	ma-def2-QZVPP	difference
$LiO_2 + O_2^- \rightarrow LiO_4^-$	-2.662	-2.560	3.8 %
$LiO_4^- \rightarrow {}^3O_2 + Li(O_2)^-$	+3.142	+3.105	1.1 %
$LiO_4^- \rightarrow {}^3O_2 + Li^0(O_2)^-$	+2.618	+2.602	0.6 %
$({}^3\Sigma - {}^1\Delta)$ O_2 gap	+0.962	+0.944	1.8 %

Supplementary Table 3: Reaction energy differences for the $MO_2+MO_2 \rightarrow M_2O_2 + O_2$

Cation	Vacuum	Et_2O	CH_3CN
Peroxide product $M^+O_2^{2-}M^+$			
Li^+	-0.79	-0.30	-0.14
Na^+	-0.29	+0.24	+0.40
K^+	+0.09	+0.62	+0.79
Superoxide product $M^0O_2^-M^+$			
Li^+	+1.65	+2.11	+2.29
Na^+	+0.76	+1.43	+1.89
K^+	+0.76	+2.04	+2.27